



HAL
open science

Characterization of water transport and flooding conditions in polymer electrolyte membrane fuel cells by electrochemical pressure impedance spectroscopy (EPIS)

Anantrao Vijay Shirsath, Caroline Bonnet, Divyesh Arora, Stéphane Raël,
François Lopicque

► To cite this version:

Anantrao Vijay Shirsath, Caroline Bonnet, Divyesh Arora, Stéphane Raël, François Lopicque. Characterization of water transport and flooding conditions in polymer electrolyte membrane fuel cells by electrochemical pressure impedance spectroscopy (EPIS). *International Journal of Heat and Mass Transfer*, 2022, 190, pp.122767. 10.1016/j.ijheatmasstransfer.2022.122767 . hal-03827535

HAL Id: hal-03827535

<https://hal.science/hal-03827535>

Submitted on 24 Oct 2022

HAL is a multi-disciplinary open access archive for the deposit and dissemination of scientific research documents, whether they are published or not. The documents may come from teaching and research institutions in France or abroad, or from public or private research centers.

L'archive ouverte pluridisciplinaire **HAL**, est destinée au dépôt et à la diffusion de documents scientifiques de niveau recherche, publiés ou non, émanant des établissements d'enseignement et de recherche français ou étrangers, des laboratoires publics ou privés.



Distributed under a Creative Commons Attribution - NonCommercial - NoDerivatives 4.0 International License

Characterization of water transport and flooding conditions in polymer electrolyte membrane fuel cells by electrochemical pressure impedance spectroscopy (EPIS)

Anantrao Vijay SHIRSATH, Caroline BONNET, Divyesh ARORA, Stéphane RAËL¹, François LAPICQUE*

Université de Lorraine, CNRS, LRGP, F-54000 Nancy, France

¹ Université de Lorraine, GREEN, F-54000 Nancy, France

Abstract:

The manuscript focuses on the use of pressure induced impedance spectroscopy (EPIS) to investigate transport phenomena in a membrane fuel cell in the presence of liquid water. A step-by-step approach is used to differentiate the different phenomena. Experiments were conducted in oxygen or air, at different currents, flowrates or relative humidities, with different GDLs (with or without MPL and PTFE) and in new or aged assemblies. In the presence of oxygen, over the whole frequency range (1-1000 mHz), the greater the amount of liquid water, the higher the impedance modulus. This observation is accentuated with the absence of MPL, PTFE, and for an aged assembly. For frequencies below 10mHz, water transport is problematic, while gas transport appears impacted for frequencies above 100mHz. For a less efficient GDL with a large water excess, the phase shift is shifted toward negative values over 100mHz. In the presence of air, diffusion is superimposed on the previous phenomena: increase in the EPIS modulus at high frequencies and strong decrease in the phase shift. In the case of air and conditions close to flooding, the EPIS modulus increases severely in the range 0.1-1Hz and the phase shift increases strongly in positive values between 1-30mHz.

Keywords: Electrochemical pressure impedance spectroscopy; electrochemical impedance spectroscopy; membrane fuel cells; gas transport; gas diffusion layers; flooding

*Corresponding author: francois.lapicque@univ-lorraine.fr

1. Introduction

Amongst the various strategies to mitigate CO₂ emissions and global warming, hydrogen-based energy [1,2] and proton exchange membrane fuel cells (PEMFC) can be considered as promising routes for many day-to-day applications [3,4]. PEMFCs comprise a membrane electrode assembly (MEA) comprising a polymer electrolyte membrane (PEM) with catalyst layers (CL) and two gas diffusion layers (GDL) on either side of it. The membrane is often of Nafion™ or comparable ionomers, and has either side coated electrodes loaded with platinum catalyst [5,6]. GDLs are based upon either carbon cloth or carbon paper. Their main role is to facilitate the distribution of reacting gases to the catalyst layer, to act as a conducting medium for electron transfer from the MEA to the bipolar plates, to provide support and durability to the MEA [6] and to improve water management.

First GDL generations had no hydrophobic treatment, which usually led to poorly efficient water transport in the various parts of the fuel cell : accumulated liquid water resulted in hindered transport of reacting gases and reduced access of the reacting gases to the catalytic sites, decreasing significantly the fuel cell performance. In addition, excessive presence of liquid water was shown to cause irreversible damages to the MEA, such as carbon corrosion, and washing out of the catalyst [7-9]. To improve gas distribution and avoid flooding in the fuel cell, most GDL microporous substrates (MPS) are now coated with a microporous layer (MPL) consisting of fine carbon-based microparticles and graphitized resins, and containing polytetrafluoroethylene (PTFE) as a hydrophobic binder. The MPL facing the catalyst layer acts as an intermediary region in the cell and favours uniform distribution of reactant gases [8, 10-12]. Moreover, MPLs were shown to enhance the water transport across the membrane from the cathode to the anode [7] and toward the cathode outlet through the bipolar plate, thus reducing occurrence of water flooding. The different

surface properties of the MPL in comparison to those of the MPS induce a discontinuity in the liquid water saturation levels, increasing some more water rejection rates [13]. Finally, the MPL can diminish the electrical contact resistance between the MPS and the electrode, while boosting the fuel cell performance by lowering kinetic and mass transport losses [7,14,15].

Degradation of the GDL affects water management and results in the decrease in the fuel cell performance, which can be diagnosed and characterized using various electrochemical techniques. Amongst them, electrochemical impedance spectroscopy (EIS) establishes a relationship between current and potential fluctuations depending on the frequency varied in a quite broad range. EIS showed its efficiency to characterize charge transport in the cell components and transfer to the electrode surface, for frequency larger than 1 Hz. Mass transport limitations can also be evidenced below a few Hz, however in most cases, the different mass transport processes with comparable time constants [16-19], cannot be distinguished from one another. It was therefore suggested to use a non-electrical variable in the fluctuation-based technique e.g. concentration as in [9] or gas pressure [20] coupled with an electrical variable e.g. cell voltage, in order to allow differentiation of the various transport phenomena in the fuel cell. In particular, the phase shift behavior was observed to be linked to the dynamics of water accumulation [20]. Applying this technique to sodium-oxygen batteries, Hartmann et al. [21] could successfully highlight water transport phenomena and hydration imbalance conditions, including their effects on oxygen transport. They termed this novel technique as electrochemical pressure impedance spectroscopy (EPIS). The potential of EPIS in investigating electrochemical cells involving the presence of a gas phase was soon confirmed by simulation [22]. EPIS impedance here defined as the ratio of voltage fluctuations over back pressure oscillations $Z_{V/P}$, was successfully performed on a fuel cell using a loudspeaker to generate pressure oscillations from 1 mHz to 100 Hz [23], although the

experimental spectra were presumably subject to considerable noise. As reported previously [16,17], inducing cathode back-pressure fluctuations by means of a pressure controller within the frequency range 1 mHz -1 Hz, and observing the associated cell voltage response, can produce clean EPIS spectra with valuable information on transport phenomena, such as gas transport control or sluggish evacuation of liquid water.

In complement to the preliminary results [16,17], the present study aimed to observe and characterize water transport, depending on the hydration state in the cell and its water management capability. In the various designed experiments, hydrogen was always fed dry to the cell. The first three series of experiments were conducted with pure oxygen to avoid interference from O₂ diffusion in N₂ observed in the range 20 mHz - 1 Hz [16]. The step-by-step approach followed, enabled a better understanding of EPIS spectra, making it possible to evidence water-involving phenomena and related issues in PEMFC. More precisely, first tests were conducted with a fresh MEA in wet conditions ($j = 1.0 \text{ A cm}^{-2}$, RH = 100% with the usual gas flow rate at the cathode), and compared to dry conditions ($j = 0.2 \text{ A cm}^{-2}$ and RH = 20%) to evidence the presence of liquid water. These experiments with a fresh MEA provided with a commercial MPL-coated GDL at both electrodes, were identified as a reference case for further comparison. Afterward, an aged MEA with the same specifications, and having been submitted to NEDC cycling operations [24], was tested in a second step under EPIS with pure oxygen. Thirdly, a fresh MEA with a commercial MPL-coated GDL at the anode, and a GDL provided with or without an MPL at the cathode side, was used with far lower gas flow rate of O₂ in the cathode to investigate more extreme hydration conditions in the cell. Finally, a fourth series of tests was conducted with air to investigate more real operating conditions of a fuel cell with very different hydration states and water management capacities.

2. Materials and methodology

The laboratory test bench for application and validation of EPIS for a 100 cm² UBzM single PEM fuel cell was previously described [17]. In this work, EPIS has been applied to a single cell 100 cm² PEMFC with a ‘symmetric’ arrangement i.e. with identical GDLs at the cathode and at the anode, as well as in an ‘asymmetric’ arrangement i.e. with different GDLs in the two FC compartments. In all cases, the MEA comprised a 20 µm thick Gore membrane and two gas diffusion electrodes (GDE) with a Pt loading at 0.4 mg cm⁻² at the cathode and 0.1 mg cm⁻² at the anode. GDLs (Sigracet, Germany) were of either 29 BC grade – a recent grade comprising an MPL, or 34 BA without MPL but whose microporous substrate was rendered more hydrophobic upon PTFE treatment, or 29 AA, an MPL-free GDL but whose microporous layer was not PTFE-treated. The last GDL is to exhibit problematic water management. A Sigracet 29 BC grade GDL was placed at the anode at all tests, irrespective of the experimental conditions. Table 1 shows the different GDLs used during experimentations and their transport properties.

In the following text, MEA denotes the above membrane electrode assembly sandwiched between two GDLs. The MEA could be a freshly matured assembly or aged after 1000 hours NEDC cycling operation [27] emulating FC operation in urban and suburban drive. It was formerly shown by EIS measurements [28] that such ageing substantially degraded the mass transfer properties of the GDL, in particular its capability in water management.

The experimental bench was designed to supply pure oxygen or air to the cathode, depending on the planned operating conditions. During operation, hydrogen was always fed dry to the fuel cell anode, whereas the cathode inlet gas was humidified at controlled relative humidity (RH_c) fixed either at 20 or 100%. To favour high hydration with possible water flooding, the cathode inlet RH_c and the current density were increased. It was previously observed that the fuel cell is prone to

accumulate excessive liquid water at high current density which explains that both the current density and RHC were changed for these two cases. The amounts of water collected from the condensers at 5°C at the cell outlets gave access to the fraction of liquid water in the gases at the cell outlet.

Four series of experiments were carried out. The gas flow rates were fixed to allow excess in the molar amounts of reacting gases: stoichiometry factor λ_{H_2} was fixed at 1.2, and unless specified, λ_{O_2} varied from 4 to 11.91 for pure oxygen and $\lambda_{O_2} = 2.5$ was for air. The flow rate of oxygen at $\lambda_{O_2} = 11.91$ was the same as the one with air at $\lambda_{O_2} = 2.5$ considering 21% O₂-containing air. The current density was in the range 0.2 – 1 A cm⁻². The conditions for the four experiment series presented here are reported in Table 2.

Pressure sensors (Keller instruments) monitored the inlet and outlet pressures of both cell compartments. For EPIS measurements, pressures at both cathode and anode outlets were first fixed at a steady level $\bar{P}_{out} = 150$ mbars using Brooks Instruments pressure controllers installed at each gas stream outlet. Then, while keeping the anode back-pressure constant at \bar{P}_{out} , sinusoidal pressure fluctuations of the cathode back-pressure were applied with amplitude ΔP_{out} and frequency f , resulting in fluctuations of the cell voltage to be continuously monitored at constant current density. The frequency-domain considered for the study was 1 mHz to 1 Hz. In addition, for each frequency, the pressure amplitude was selected to allow a linear relationship between pressure and voltage fluctuations, condition required for use of Laplace transform and impedance spectroscopy, and to allow response voltage amplitude larger or equal to 1 mV. A defined set of periods at a given frequency was recorded; this set was termed as acquisition. Usually, 10 periods per acquisition were recorded at 10 mHz and above, and only three for lower frequencies [17]: this

procedure enabled to generate a comparable mean period per acquisition for each recorded signal, and to reduce the noise level on the voltage signal before Fourier analysis.

3. Results and discussion

The three first sets of experiments were carried out with pure oxygen to avoid contribution of diffusion phenomenon and allow evidence of water transport control. Based on the reported time constants for liquid water transport in the GDL and in the PEM at 3 min and 25 s respectively [28], it was hypothesized that the water transport could be evidenced in the low-frequency domain of the spectra ($f < 50$ mHz), because of the far larger diffusivity and viscosity of liquid water rendering its transport far slower than those for gases. Further, to observe more complex conditions, experiments with air in the presence of liquid water in excess have been carried out and reported.

3.1 Evidence of water transport in the GDL (Experiments nr. 1)

The fuel cell was operated with pure oxygen and using a fresh 29 BC GDL at the cathode, under “dry” or “wet” conditions: “dry” corresponds to operation at 0.2 A cm^{-2} with RH_c fixed at 20%, and “wet” it for operation at 1 A cm^{-2} with fully humidified oxygen ($\text{RH}_c=100\%$). In “dry” conditions, the fraction of liquid water leaving the cathode compartment at the fuel cell temperature was found at 22% whereas it attained 56% under “wet” conditions. Figure 1a shows a comparison between the impedance modulus obtained for “dry” and “wet” conditions. The modulus of EPIS impedance in “wet” conditions was measured to be on average 40% larger than that in “dry” conditions in the whole frequency range investigated (Figure 1a), in all cases at a moderate significance i.e. below $1 \mu\text{V Pa}^{-1}$. The change in EPIS modulus for low frequencies was attributed to liquid water transport in the porous FC structures as previously evidenced in nearly flooding conditions [17]. For frequencies beyond 10 mHz, the EPIS modulus was shown to slightly decrease

(Figure 1a). It has been previously observed that EPIS impedance in this frequency domain was not directly caused by water transport but was the hindering consequence of its presence on gas transport in the FC porous layers.

The phase shift had very little positive values at 1 mHz and followed a slightly decreasing trend until reaching a minimum at intermediate frequencies. However, in “wet” conditions, the phase shift at 1 mHz is higher (6°) than in “dry” conditions (3°): the moderate difference is observed up to 10 mHz. Moreover, in the higher frequency domain (100 mHz to 1 Hz), the phase shift for “dry” conditions is more negative (-15°) than in “wet” conditions (-7.5°). Further investigations would be needed to understand better the role of phase shift in the characterization of excess water accumulation or water transport.

These results show that EPIS is sensitive towards water transport control in the fuel cell. In spite of the good aptitude of 29 BC GDL in water management, the increased amount of liquid water at high current density and humidification conditions render water transport phenomena more troublesome.

3.2 Evidence of water transport control for an aged MEA (Experiments nr. 2)

Experiments with an MEA (including the GDLs) aged by cycling operations were conducted to investigate the flooding conditions since such an MEA was shown to exhibit far poorer water management capability, and thus is significantly prone to flooding. The MEA was taken from a 3-cell stack submitted to NEDC cycling protocol with a cumulative operation time around 1000 h [24,29]. The difference of the two MEA performances is clearly shown in Figure 2a with fully humidified oxygen; in particular, voltage could not be measured beyond 0.6 A cm^{-2} with the aged MEA, whereas the freshly matured MEA allowed a voltage near 0.5 V at 1 A cm^{-2} . Therefore, EIS

and EPIS spectra were recorded at 0.4 A cm^{-2} only to avoid total collapse of the aged MEA. The ohmic resistance estimated at high frequencies, was 70% larger with the aged MEA (Figure 2b), likely due to the appreciable delamination of the various FC layers under cycling conditions [24, 29]. Whereas the spectrum of the fresh MEA consisted of two loops for charge and mass transfer of a restricted importance, the spectrum recorded with the aged MEA exhibits a single huge loop with an overall impedance nearly four times larger than for the fresh MEA (Figure 2b). EIS Bode plots (Figure 2c) exhibited comparable profiles for the two MEAs at high frequencies, and monotonous increases in modulus and phase below 10Hz. In spite of the very different impedances under 10 mHz shown by EIS, the two Bode plots do not indicate precisely on the nature of mass transfer control in the fuel cell.

Figure 3a shows the spectra of EPIS impedance modulus for the aged and the fresh MEA. A two times increase in the impedance modulus for frequencies lower than 100 mHz can be observed with the the aged MEA, attaining a maximum near $1 \mu\text{V Pa}^{-1}$ at 10 mHz. The significant increase in the impedance values in the lower frequency domain expresses the stronger control from water transport due to troublesome water evacuation away from the catalytic sites, causing excessive water buildup in the GDL structure. Comparison with the EPIS profiles under reference “dry” and “wet” conditions shown in Figure 1 and reported in dotted line in Figure 3, illustrates the specific effect of poorer water management of the aged MEA, in particular on EPIS modulus: at low frequencies, water transport is more problematic, and at higher frequencies, gas transport – here mainly by convection - is more hindered by the liquid water present. The increment in impedance modulus for frequencies greater than 100 mHz might express more troublesome gas transport due to droplet formation limiting the cross-sectional area available to gases together with less even gas distribution.

However, the phase shift was found to exhibit very comparable variations for the two cases (Figure 3b). This fact could be not interpreted up to now since the phase shift behavior might be linked to the dynamics of water accumulation [20]. The slightly larger phase shift values for $f < 10$ mHz with the aged MEA might be attributed to water transport limitations, but this effect is here of a minor significance.

The degradation in aged GDL known to favour flooding conditions to occur in the cell structure, was found to concern mainly its MPL. The MPL was shown by SEM observation to be locally torn off from the microporous substrate, as clearly evidenced on the photograph (Figure 4). Thus the degraded GDL is more prone to retain liquid water in the MPL-deprived areas of a far lower hydrophobicity. The puddles formed in the MPS likely reduce the path cross section for gas transport in the GDL porous structure to access the catalytic sites. Furthermore, gas is to flow predominantly through the GDL region deprived of the MPL: both phenomena result in far lower FC performance. SEM analysis is consistent with the above EIS and EPIS spectra and confirms the hypothesis of more problematic mass transfer of liquid water and its accumulation in the fuel cell structure.

To investigate further the effect of absence of the MPL layer and hydrophobic treatment, experiments with different types of GDLs were carried out.

3.3 Effect of the GDL type on water management (Experiments nr. 3)

Following the studies mentioned in the introduction, GDLs coated with an MPL e.g. 29 BC, allow significant flooding conditions in the fuel cell to be avoided. On the contrary, extreme flooding conditions should be visualised by EPIS with GDLs with compromised water management capacity and operated at reduced stoichiometry in wet conditions. The three GDLs described in Table 1

were then tested in the fuel cell cathode fed by pure oxygen at $\lambda_{O_2} = 4$, with RH = 100% and $j = 1$ A cm⁻². This set of operating conditions is to allow highly pronounced flooding conditions: as a matter of fact, the fraction of liquid water at the cell outlet over the water present was found equal to 82%. Although the residence times of gas and liquid water are likely different in the fuel cell, the high fraction value expresses qualitatively the significance of liquid water in the cell. Lower stoichiometric factors could not successfully be tested at this current density with the two MPL-free GDLs placed at the cathode.

For EPIS impedance modulus (Figure 5a), a clear trend can be seen all over the spectra with 29 AA exhibiting the highest impedance modulus followed by 34 BA and 29 BC: EPIS modulus is nearly two times larger for 29 AA than with 29 BC for frequencies below 80 mHz. The difference although of a lower significance, is in the range 45-70% in the higher frequency domain. As in the previous sub-section, EPIS spectra for reference “wet” conditions (Figure 1) are given in Figure 5 in dotted lines for comparison. The higher liquid fraction in the cell with $\lambda_{O_2} = 4$ with 29 BC causes a visible increase in the EPIS modulus from the reference case $\lambda_{O_2} = 11.9$ in the whole frequency domain, revealing the effect of oxygen stoichiometry on liquid water transport at lower frequencies, and more strongly hindered gas transport in the GDL at higher frequencies. Besides, EPIS modulus with 34 BA was 10-15% larger than that with the MPL-provided GDL: the 34 BA GDL exhibits an intermediate behaviour between more recent MPL-coated 29 BC layer and 29 AA, deprived of water repellent materials. Through careful examination, it appears that the impedance modulus with 29 BC remains nearly constant in the 1 – 100 mHz range whereas with 34 BA and 29 AA, there is an increase in the impedance modulus at low frequencies. This trend might be attributed to the accumulation of excessive liquid water or near-flooding conditions in the lower frequency region.

On the other hand, a trend seems to emerge in the whole frequency domain with 29 AA showing more significant – positive or negative - phase shifts than with the other two GDLs (Figure 5b). Together with EPIS modulus, more positive phase shifts below 10 mHz might express nearly flooding conditions in the fuel cell with the PTFE-free 29 AA layer. For frequencies larger than 40 mHz, more negative phase shifts with this basic GDL may indicate on more difficult flow of oxygen in the fuel cell structure, with a minimum near -18° at 200 mHz, in comparison to the minima near -12° exhibited by the two other GDLs. Moreover, the dotted line for 29 BC with $\lambda_{O_2} = 11.9$ illustrates the effect of aggravated water management upon reduction in the oxygen stoichiometry with the same GDL, in particular for gas transport hindrance for frequencies larger than 30 mHz.

3.4 Operating with air and excess water accumulation (Experiments nr. 4)

In practice, fuel cell cathodes are usually fed with air, for which gas diffusion and convection occur simultaneously: these more realistic conditions have been investigated in this section. The FC was thus operated with air either at $j = 1 \text{ A cm}^{-2}$ and $\text{RH}_c = 100\%$ (for wet conditions), or at 0.2 A cm^{-2} and $\text{RH}_c = 20\%$ for dry conditions. The fuel cell was equipped with an MEA with 29 BC grade GDL at the anode and a 34 BA grade GDL at the cathode. Experiments with 29 AA GDL could not be carried out for these operating conditions because of the rapidly decaying cell voltage in preliminary tests. For comparison purpose, the reference “wet” test with 29 BC GDL was also carried out, here with air ($\lambda_{O_2} = 2.5$). As expected, the performance of the fuel cell with 34 BA GDL is visibly affected by air relative humidity, with voltage difference being near 60 mV at 0.2 A cm^{-2} but attaining 300 mV at 1 A cm^{-2} (Figure 6a), expressing the poor water management of the 34-BA GDL. This large difference in fuel cell performance was confirmed by EIS spectra of the three MEA operated under the above defined conditions (Figure 6b), with two well-defined

loops with 29 BC and only one huge loop covering charge and mass transfers with the 34 BA GDL operated in wet conditions. For 34 BA operated in dry condition, the charge transfer loop is far larger than that in the spectrum with 29 BC because of the very lower current density. Besides, the mass transfer loops of the two MEAs are comparable importance owing to sort of compensation effect of different current density and different capability in water management.

Figure 7a shows compared variations of EPIS impedance modulus in wet and dry conditions of the cell investigated and operated with the two GDL. As seen in the Figure, the impedance modulus exhibits different profiles in the 1 - 10 mHz domain, being at 2.4 and 0.75 $\mu\text{V Pa}^{-1}$ respectively at 1 mHz in wet and dry conditions with 34 BA: this difference is illustrated by the blue area in the Figure. Corresponding modulus was only near 0.5 $\mu\text{V Pa}^{-1}$ with 29 BC GDL in wet conditions (Figure 7a), confirming the positive effect of the MPL. For frequencies larger than 50 mHz, the occurrence of oxygen diffusion in nitrogen is clearly expressed by large peaks in EPIS modulus with a maximum in the range 200 – 500 mHz: this is illustrated by the area in red in Figure 7a . The behaviour of the MEA provided with 34 BA GDL was strongly affected by the hydration state in the cell, with nearly four times larger maximum in EPIS modulus under wet conditions. Although operated with 29 BC in wet conditions, the MEA seems to little far less hindered by mass transfer, in accordance with EIS spectra (Figure 6b). However, contrary to EIS, EPIS showed that water transport at low frequency is little problematic with 29 BC and gas transport rates are moderately affected by the presence of liquid water, with a flat maximum of the modulus at 4.4 $\mu\text{V.Pa}^{-1}$ at 400 mHz, more than ten times lower than the corresponding peak with 34 BA in the cell presumably running in nearly flooding conditions. In the frequency domain 10 to 100 mHz, the increase in impedance modulus likely corresponds to the superimposition of liquid and gas

mass transport phenomena whose spectral significances partly overlap: this region is coloured in green in the Figure.

The phase shift of EPIS impedance (Figure 7b) starts at nearly 0° at 1 mHz with 34 BA in dry conditions and 29 BC (wet), then regularly decreases to -200° or so at 1 Hz, as previously observed in numerous cases [16, 17] with 29 BC GDL. However, in wet conditions with 34 BA, the phase shift starts very positive (170°) to end at approx. -250° at 1 mHz (Figure 7b). This dramatic increase in the phase shift in the lower frequency domain confirmed by replicate experiments, would be the fact of flooding conditions due to poor water management of the MPL-deprived GDL. In comparison, the positive phase shift at low frequency observed as little significant with O_2 operation (Figure 5), seems to be strongly increased with air. Although nitrogen and oxygen density and viscosity differ by less than 15%, it cannot be excluded that formation of water droplets in the microscopic porous medium could be affected by the nature of the gas. Further fundamental work would be required to confirm or amend this hypothesis, still speculative up to now. Moreover, the decrease in phase shift beyond -200° in the high frequency region might reflect more significant gas transport control due to the presence of excess liquid water, as reported above in Section 3.3.

4. Conclusion

In this work, an EPIS investigation of a highly hydrated fuel cell was carried out under gas and liquid transport limitations due to the presence of liquid water. Moreover, to better evidence the water transport control, most EPIS measurements were carried out with pure oxygen fed to the cathode to avoid the occurrence of diffusion phenomena, which were previously shown to result in strong changes in the modulus and phase shift of EPIS impedance. Several cases were compared e.g. “dry” or “wet” conditions - with different current density and relative humidity at the cathode

inlet - or the water management ability of the cathode GDL through its state of health, the presence of a microporous layer or PTFE treatment of its macroporous substrate. Mass transport control from liquid water in the porous structure of the fuel cell was revealed by the increase in EPIS modulus in the 1 - 10 mHz frequency domain. Moreover for nearly flooding conditions, the phase shift decreasing trend with the frequency was shown to be positively shifted for frequencies lower than 10 mHz. In addition, gas transport previously evidenced from 20 mHz, exhibits higher EPIS modulus under high hydration of the cell or poorer water management conditions, because of the reduced cross sectional area available for gas flow in the fuel cell structure. Further tests under air operation confirmed the trend, the additional huge signature of gas diffusion in terms of EPIS modulus and phase shift could be observed from 20 mHz: in comparison with “dry conditions”, operating in nearly flooding conditions results in five time increase in EPIS modulus at 200 mHz. Finally, the frequency domains of rate-controlling transport of gases and liquid, likely overlap in the range 10 – 100 mHz. The overall work confirms the interest in EPIS for mass transport investigation in the presence of liquid water, whereas EIS has to be preferred for faster phenomena e.g. charge transport or transfer.

In spite of recent modelling work of EPIS [30], the present work focused on nearly flooding conditions, would need further theoretical work to better understand the physical meaning of particular features of EPIS impedance such as very different profiles of impedance modulus from 10 mHz, or highly positive phase shifts for frequency below 20 mHz.

Conflict of interest

The authors declare that there is no conflict in interest.

Acknowledgment:

The authors would like to thank the ANR-EPISTEL (ANR-17-CE05-0031) and DFG for the Ph.D. grant support for A.V. Shirsath and the funding of the overall project.

Literature cited

- [1] IPCC, Summary for Policymakers. Global Warming of 1.5°C., in: Glob. Warm. 1.5°C. An IPCC Spec. Rep. Impacts Glob. Warm. 1.5°C above Pre-Industrial Levels Relat. Glob. Greenh. Gas Emiss. Pathways, Context Strength. Glob. Response to Threat Clim. Chang., 2018. <https://doi.org/10.1017/CBO9781107415324>.
- [2] C. Acar, I. Dincer, The potential role of hydrogen as a sustainable transportation fuel to combat global warming, *Int. J. Hydrogen Energy* 45 (2020) 3396–3406.
- [3] A.G. Olabi, F.N. Khatib, A. Baroutaji, T. Wilberforce, J.G. Carton, Z. El-Hassan, A. Al Makky, Developments of electric cars and fuel cell hydrogen electric cars, *Int. J. Hydrogen Energy* 42 (2017) 25695–25734. <https://doi.org/10.1016/j.ijhydene.2017.07.054>.
- [4] W.R.W. Daud, R.E. Rosli, E.H. Majlan, S.A.A. Hamid, R. Mohamed, T. Husaini, PEM fuel cell system control: A review, *Renew. Energy*. 113 (2017) 620–638. <https://doi.org/10.1016/J.RENENE.2017.06.027>.
- [5] J. Larminie, A. Dicks, *Fuel Cell Systems Explained*, John Wiley Sons Ltd, Atrium, South Gate, Chichester, West Sussex PO19 8SQ, Engl. (2003) 406. <https://doi.org/10.1002/9781118878330>.
- [6] F. Lopicque, M. Belhadj, C. Bonnet, J. Pauchet, Y. Thomas, A critical review on gas diffusion micro and macroporous layers degradations for improved membrane fuel cell durability, *J. Power Sources* 336 (2016) 40–53. <https://doi.org/10.1016/j.jpowsour.2016.10.037>.
- [7] T. Kim, S. Lee, H. Park, A study of water transport as a function of the micro-porous layer arrangement in PEMFCs, *Int. J. Hydrogen Energy* 35 (2010) 8631–8643.

<https://doi.org/10.1016/j.ijhydene.2010.05.123>.

- [8] J.H. Nam, K.J. Lee, G.S. Hwang, C.J. Kim, M. Kaviany, Microporous layer for water morphology control in PEMFC, *Int. J. Heat Mass Transf.* 52 (2009) 2779–2791.
<https://doi.org/10.1016/j.ijheatmasstransfer.2009.01.002>.
- [9] A. Sorrentino, T. Vidakovic-Koch, R. Hanke-Rauschenbach, K. Sundmacher, Concentration-alternating frequency response: A new method for studying polymer electrolyte membrane fuel cell dynamics, *Electrochim. Acta* 243 (2017) 53–64.
<https://doi.org/10.1016/j.electacta.2017.04.150>.
- [10] M.S. Ismail, T. Damjanovic, D.B. Ingham, L. Ma, M. Pourkashanian, Effect of polytetrafluoroethylene-treatment and microporous layer-coating on the in-plane permeability of gas diffusion layers used in proton exchange membrane fuel cells, *J. Power Sources* 195 (2010) 6619–6628. <https://doi.org/10.1016/j.jpowsour.2010.04.036>.
- [11] K. Jiao, X. Li, Water transport in polymer electrolyte membrane fuel cells, *Prog. Energy Combust. Sci.* 37 (2011) 221–291. <https://doi.org/10.1016/j.peccs.2010.06.002>.
- [12] U. Pasaogullari, C.Y. Wang, Two-phase transport and the role of micro-porous layer in polymer electrolyte fuel cells, *Electrochim. Acta* 49 (2004) 4359–4369.
<https://doi.org/10.1016/j.electacta.2004.04.027>.
- [13] F.S. Nanadegani, E.N. Lay, B. Sunden, Effects of an MPL on water and thermal management in a PEMFC, *Int. J. Energy Res.* 43 (2019) 274–296.
<https://doi.org/10.1002/er.4262>.
- [14] C.J. Tseng, S.K. Lo, Effects of microstructure characteristics of gas diffusion layer and microporous layer on the performance of PEMFC, *Energy Convers. Manag.* 51 (2010)

677–684. <https://doi.org/10.1016/j.enconman.2009.11.011>.

- [15] S.M. Mahnama, M. Khayat, Three dimensional investigation of the effect of MPL characteristics on water saturation in PEM fuel cells, *J. Renew. Sustain. Energy*. 9 (2017) 014301. <https://doi.org/10.1063/1.4974339>.
- [16] A.V. Shirsath, S. Raël, C. Bonnet, L. Schiffer, W. Bessler, F. Lopicque, Electrochemical pressure impedance spectroscopy for investigation of mass transfer in polymer electrolyte membrane fuel cells, *Curr. Opin. Electrochem.* 20 (2020) 82–87. <https://doi.org/10.1016/j.coelec.2020.04.017>.
- [17] A.V. Shirsath, S. Raël, C. Bonnet, F. Lopicque, Electrochemical pressure impedance spectroscopy applied to polymer electrolyte membrane fuel cells for investigation of transport phenomena, *Electrochim. Acta* 363 (2020) 137157. <https://doi.org/10.1016/j.electacta.2020.137157>.
- [18] W. Schmittinger, A. Vahidi, A review of the main parameters influencing long-term performance and durability of PEM fuel cells, *J. Power Sources* 180 (2008) 1–14. <https://doi.org/10.1016/j.jpowsour.2008.01.070>.
- [19] A. Sorrentino, K. Sundmacher, T. Vidakovic-Koch, Polymer Electrolyte Fuel Cell Degradation Mechanisms and Their Diagnosis by Frequency Response Analysis Methods: A Review, *Energies* 13 (2020) 5825. <https://doi.org/10.3390/en13215825>.
- [20] A.M. Niroumand, W. Mérida, M. Eikerling, M. Saif, Pressure-voltage oscillations as a diagnostic tool for PEFC cathodes, *Electrochem. Commun.* 12 (2010) 122–124. <https://doi.org/10.1016/j.elecom.2009.11.003>.
- [21] P. Hartmann, D. Grübl, H. Sommer, J. Janek, W.G. Bessler, P. Adelhelm, Pressure

Dynamics in Metal – Oxygen (Metal – Air) Batteries: A Case Study on Sodium Superoxide Cells, *J. Phys. Chem. C* 2 (2014) 1461–1471.

<https://doi.org/10.1021/jp4099478>.

- [22] D. Grübl, J. Janek, W.G. Bessler, Electrochemical Pressure Impedance Spectroscopy (EPIS) as Diagnostic Method for Electrochemical Cells with Gaseous Reactants: A Model-Based Analysis, *J. Electrochem. Soc.* 163 (2016) A599–A610.

<https://doi.org/10.1149/2.1041603jes>.

- [23] E. Engebretsen, T.J. Mason, P.R. Shearing, G. Hinds, D.J.L. Brett, Electrochemical pressure impedance spectroscopy applied to the study of polymer electrolyte fuel cells, *Electrochem. Commun.* 75 (2017) 60–63. <https://doi.org/10.1016/j.elecom.2016.12.014>.

- [24] D. Arora, C. Bonnet, M. Mukherjee, S. Arunthanayothin, A. Shirsath, M. Lundgren, M. Burkardt, S. Kmiotek, S. Raël, F. Lopicque, S. Guichard, Long term study of directly hybridized proton exchange membrane fuel cell and supercapacitors for transport applications with lower hydrogen losses, *J. Energy Storage* (2020).

<https://doi.org/10.1016/j.est.2020.101205>.

- [25] M. Mukherjee, C. Bonnet, F. Lopicque, Estimation of through-plane and in-plane gas permeability across gas diffusion layers (GDLs): Comparison with equivalent permeability in bipolar plates and relation to fuel cell performance, *Int. J. Hydrogen Energy* 45 (2020) 13428–13440. <https://doi.org/10.1016/j.ijhydene.2020.03.026>.

- [26] M. Mukherjee, Characterization of gas transport phenomena in gas diffusion layers in a membrane fuel cell, PhD dissertation [in English], University of Lorraine, 2020.

<https://hal.univ-lorraine.fr/tel-03153432>.

- [27] publications.jrc.ec.europa.eu/repository/handle/JRC99115.
- [28] A.V. Shirsath, Experimental development of the electrochemical pressure impedance spectroscopy for characterization of transport phenomena in membrane fuel cells., PhD dissertation [in English], University of Lorraine, France, 2021.
- [29] D. Arora, K. Gérardin, S. Raël, C. Bonnet, F. Lapique, Effect of supercapacitors directly hybridized with PEMFC on the component contribution and the performance of the system, *J. Appl. Electrochem.* 48 (2018) 691–699. <https://doi.org/10.1007/s10800-018-1188-0>.
- [30] L. Schiffer, A.V. Shirsath, S. Raël, C. Bonnet, F. Lapique, W. Bessler, Electrochemical pressure impedance spectroscopy in a polymer electrolyte membrane fuel cell: A combined modeling and experimental analysis, accepted in *J. Electrochem. Soc.*

Table 1. GDLs used during experimentation and their properties

GDL	Thickness	Porosity [†]	Permeability* (m ²)	PTFE	MPL	Water management
29 BC	250 μm	0.77	2.8×10^{-13}	5%	Yes	Good
34 BA	280 μm	0.81	3.3×10^{-11}	5%	N.A.	Poor
29 AA	200 μm	0.84	2.44×10^{-11}	N.A.	N.A.	Very poor

*measured through-plane values [25], [†] measured dry porosity [26]

Table 2: Operating conditions used in the four series of experiments

Experiments	Gas cathode	GDL type	MEA	λ_{O_2}	j (A.cm ⁻²)	RH _c	Hydration state
1	O ₂	29 BC	Fresh	11.9	0.2 / 1	20% / 100%	“Dry” / “Wet”
2	O ₂	29 BC	Aged	11.9	0.4	100%	Wet
3	O ₂	29BC / 34 BA / 29 AA	Fresh	4	1	100%	Extremely wet
4	Air	34 BA	Fresh	2.5	0.2 / 1	20% / 100%	Extremely wet / flooding

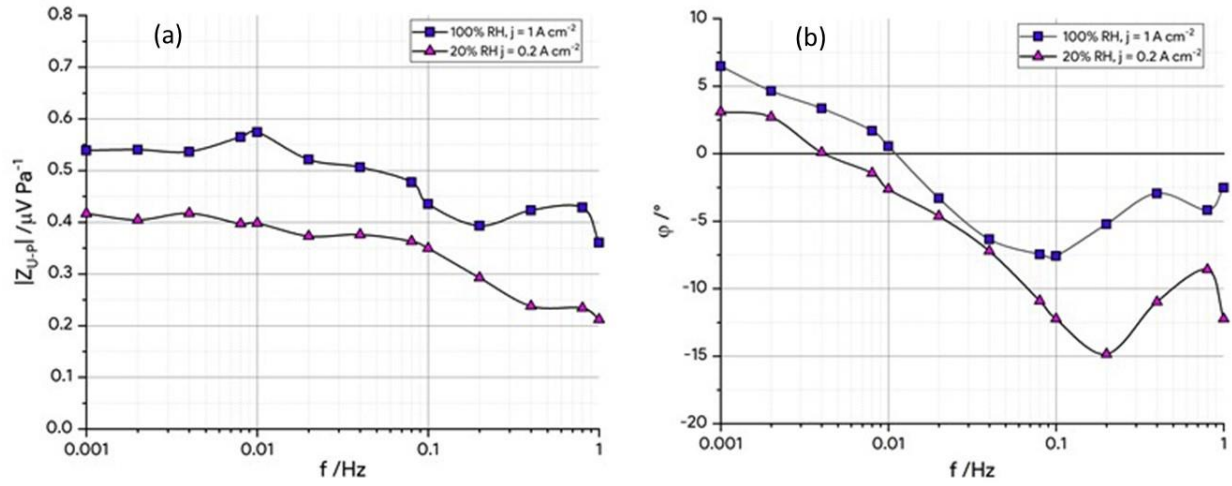


Figure 1. Comparison of (a) impedance modulus and (b) phase shift for a fresh MEA provided with 29 BC grade GDLs on both electrodes in “dry” ($\text{RH}_c = 20\%$ and $j = 0.2 \text{ A cm}^{-2}$) and “wet” ($\text{RH}_c = 100\% \text{ RH}$ and $j = 1.0 \text{ A cm}^{-2}$) conditions.

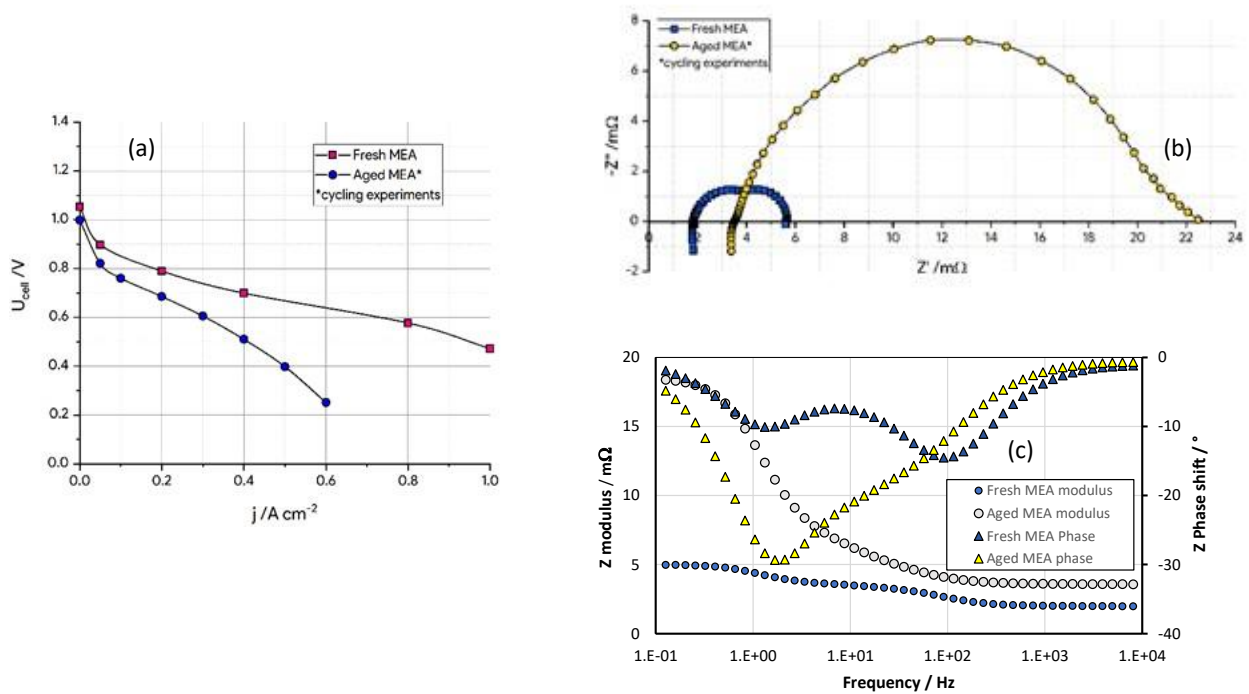


Figure 2. Comparison of fresh (beginning of life) and aged (end of life) MEA provided with 29 BC GDL at both sides with 100 % RH_c at the cathode fed with O_2 ($\lambda_{O_2} = 11.91$). a) voltage vs current density variations, b) Nyquist EIS spectra (10 kHz – 0.1 Hz) of the two cells at 0.4 $A\ cm^{-2}$. Current density amplitude = 0.04 $A\ cm^{-2}$, c) Bode plot of the spectra shown in Fig. 2b.

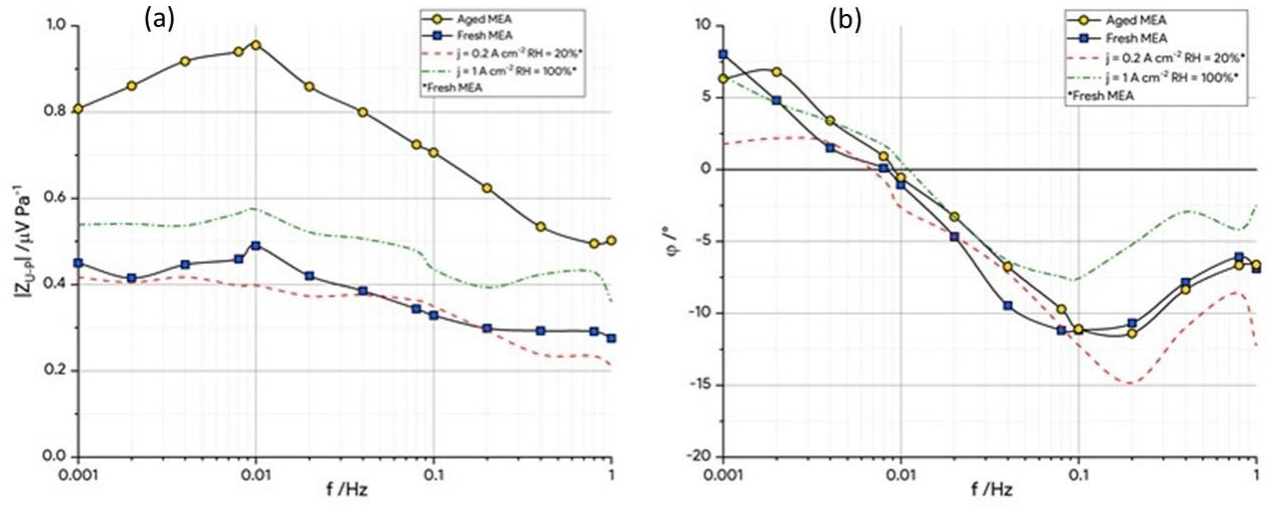


Figure 3. EPIS comparison of fresh (beginning of life) and aged (end of life) MEA provided with 29 BC GDL at both sides with 100 % RH_c at the cathode fed with O₂ ($\lambda_{O_2} = 11.91$) and operated at $j = 0.4 A cm^{-2}$: (a) impedance modulus and (b) phase shift In dotted lines for comparison, EPIS spectra for the reference “wet” and “dry” conditions (Figure 1)

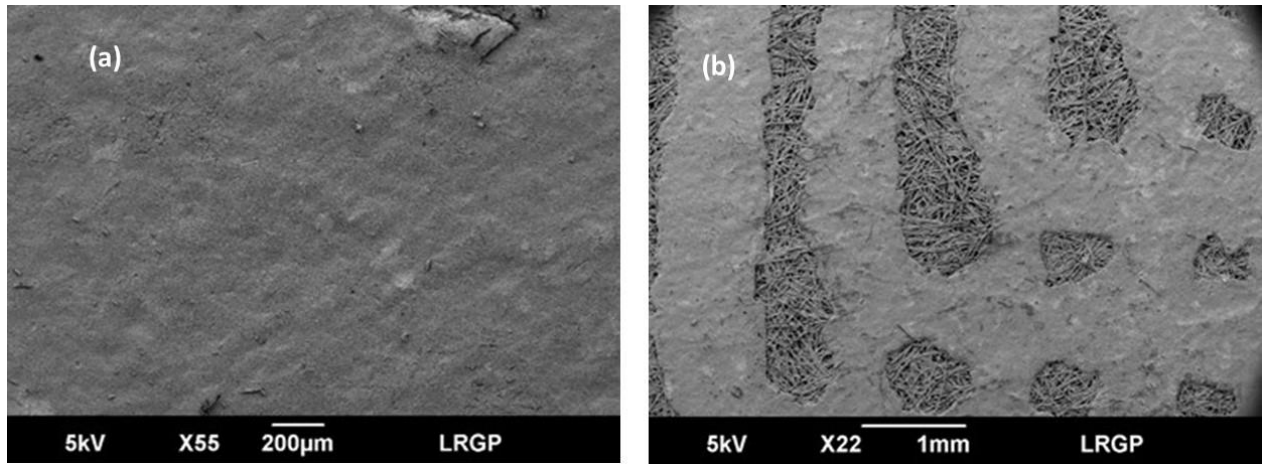


Figure 4. SEM imaging analysis of a 29 BC grade GDL in (a) fresh condition (b) after 1000 h of NEDC cycling.

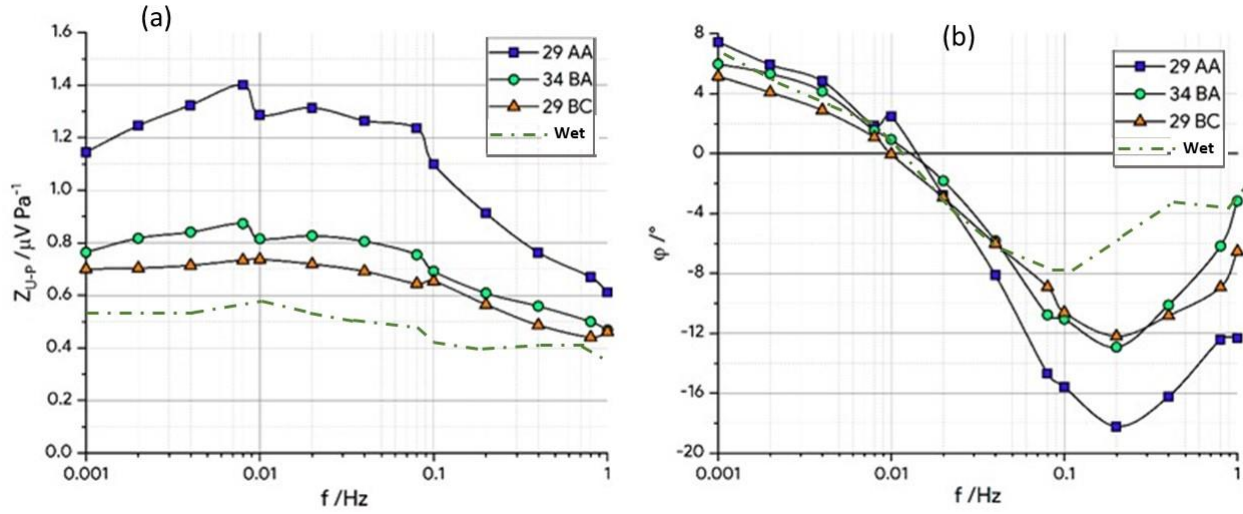


Figure 5. Comparison of (a) impedance modulus and (b) phase shift for different grades of GDL installed at the cathode of the fuel cell in wet conditions, $\lambda_{O_2} = 4$ (pure O_2), $RH_c = 100\%$ and $j = 1 \text{ A cm}^{-2}$. Spectra of the reference “wet” test of Figure 1 is also given for comparison.

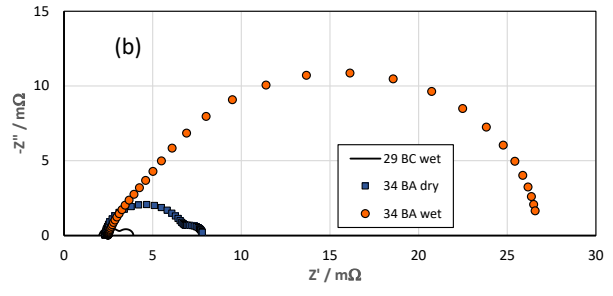
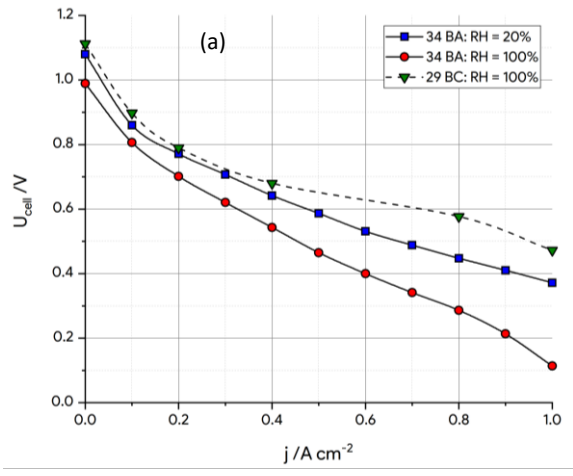


Figure 6. Performance of the fuel cell with 34 BA at the cathode fed with air ($\lambda_{\text{O}_2} = 2.5$) in which $\text{RH}_c = 20\%$ or 100% and comparison with the cell performance with 29 BC (air feed $\lambda_{\text{O}_2} = 2.5$ with $\text{RH}_c = 100\%$): a) voltage vs current density variations, b) Nyquist EIS spectra (10 kHz – 0.1 Hz) at $j = 0.2 \text{ A cm}^{-2}$ for $\text{RH}_c = 20\%$ and 1 A cm^{-2} for $\text{RH}_c = 100\%$)

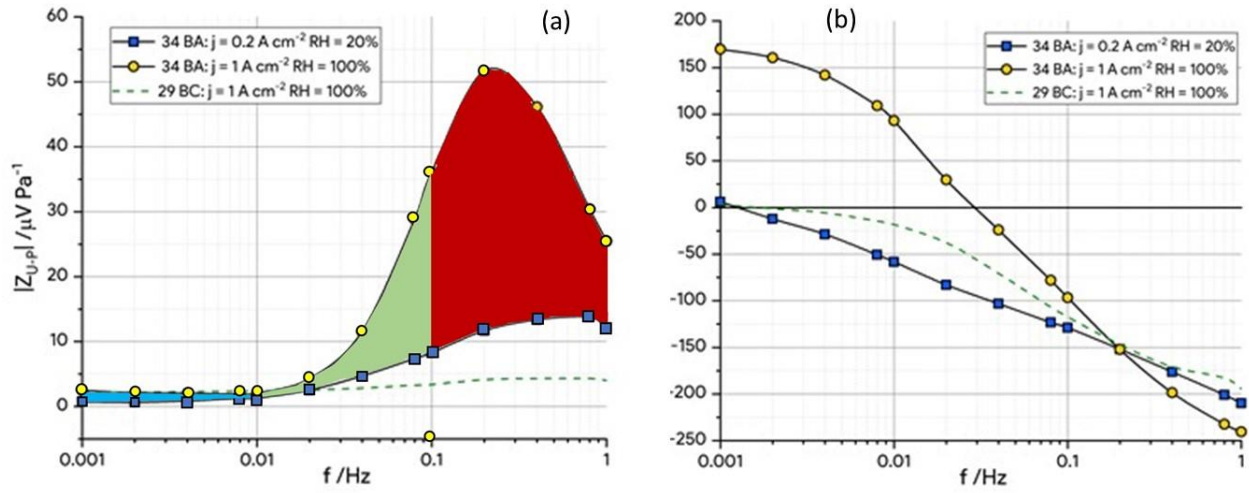
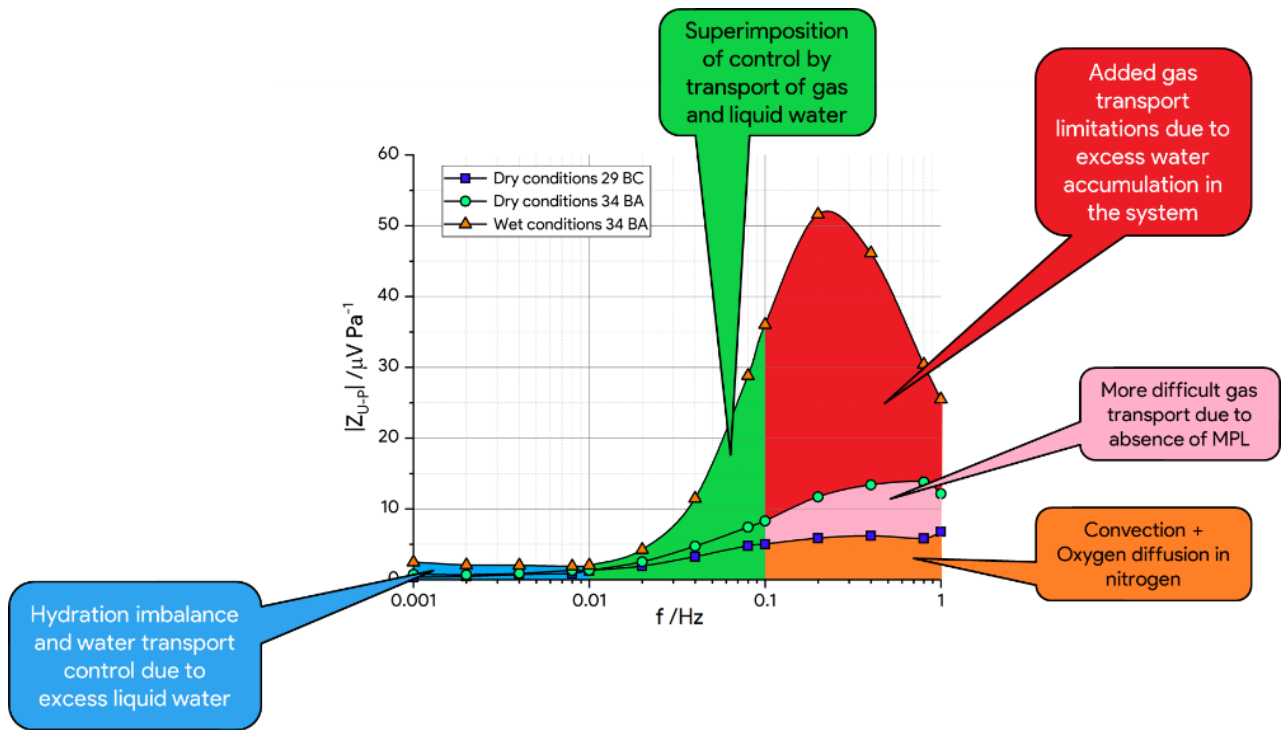


Figure 7. Comparison of EPIS (a) impedance modulus and (b) phase shift of the fuel cell fed with air ($\lambda_{O_2} = 2.5$): comparison of 34 BA used in dry conditions ($j = 0.2 \text{ A cm}^{-2}$ and $RH_c = 20\%$) or wet conditions ($j = 1 \text{ A cm}^{-2}$ and $RH_c = 100\%$), with the spectra recorded with 29 BC in wet conditions



Graphical Abstract